



ELSEVIER

Journal of Nuclear Materials 266–269 (1999) 783–787

---

---

**journal of  
nuclear  
materials**

---

---

# Measurements of flows in the DIII-D divertor by Mach probes

J.A. Boedo<sup>a,\*</sup>, R. Lehmer<sup>a</sup>, R.A. Moyer<sup>a</sup>, J.G. Watkins<sup>b</sup>, G.D. Porter<sup>c</sup>,  
T.E. Evans<sup>a</sup>, A.W. Leonard<sup>a</sup>, M.J. Schaffer<sup>a</sup>

<sup>a</sup> General Atomics, University of California, P.O. Box 85608, San Diego, CA 92093, USA

<sup>b</sup> Sandia National Laboratories, Albuquerque, NM 87185, USA

<sup>c</sup> Lawrence Livermore National Laboratory, Livermore, CA 94450, USA

---

## Abstract

First measurements of the Mach number of the background plasma in the DIII-D divertor are presented in conjunction with temperature  $T_e$  and density  $n_e$  using a fast scanning probe array. To validate the probe measurements, we compared our  $T_e$ ,  $n_e$  and  $J_{\text{sat}}$  data to Thomson scattering data and found good overall agreement in attached discharges and some discrepancy for  $T_e$  and  $n_e$  in detached discharges. The discrepancy is mostly due to the effect of large fluctuations present during detached plasmas on the probe characteristic; the particle flux is accurately measured in every case. A composite 2-D map of measured flows is presented for an ELMing H-mode discharge and we focus on some of the details. We have also documented the temperature, density and Mach number in the private flux region of the divertor and the vicinity of the X-point, which are important transition regions that have been little studied or modeled. Background parallel plasma flows and electric fields in the divertor region show a complex structure. © 1999 Elsevier Science B.V. All rights reserved.

*Keywords:* Plasma flow; DIII-D; Mach probe; Flow reversal

---

## 1. Introduction

Divertors are a critical component of existing and planned magnetic confinement fusion experiments. The role of the divertor is to provide heat and particle exhaust while allowing impurity entrainment. Impurities, mostly carbon, are present in tokamak plasmas as they are released from plasma-facing components through physical and chemical sputtering [1]; these processes also damage the divertor components. There is thus a need to understand and study divertor physics and, in particular any process, such as plasma flow, transport heat and particles to the divertor components, causing structural damage. Plasma flows can also affect particle and power fluxes [2,3] to the target plates and pumping

apparatus and therefore are critical to the design of divertors.

Indications that flows in the divertor can exhibit complex behavior have been obtained from 2-D modeling [4,5] but insofar remain mostly unconfirmed. An important phenomenon which affects flow physics is that of flow reversal. Flow reversal has been predicted analytically [6] and it is expected when the ionization source arising from neutral or impurity recycling in the divertor region is so large that the target plate, limited by the ion saturation current, cannot absorb all the particles. Reversed flow is expected to first appear near the 40 eV electron temperature contour, where the ratio of the rate coefficient for electron impact ionization to the square root of the temperature  $\langle\sigma v\rangle/T_e^{1/2}$ , is maximum and therefore the particle source becomes large. Simulations by UEDGE [4], a 2-D fluid plasma and neutral code predict flow reversal in the DIII-D divertor, approximately in regions which follow the 40 eV contour.

In order to reduce the heat and particle fluxes to the divertor target plates, a radiative divertor regime has

---

\* Corresponding author. Tel.: +1-619 455 3832; fax: +1-619 455 3586; e-mail: boedo@gav.gat.com

been proposed in which the energy and momentum of the plasma are dissipated into a large amount of neutral gas introduced in the divertor region. Cooling the plasma by collisional and atomic processes leads to detachment of the plasma from the target plates. These radiative divertor regimes have been the subject of extensive studies [7] and it has been recently proposed that the energy transport over large regions of the divertor must be dominated by convection [8] instead of conduction. It is therefore important to understand the role of the plasma conditions and geometry on determining the region of convection-dominated plasma in order to properly control the heat and particle fluxes to the target plates and hence, divertor performance.

Some efforts have been made to characterize plasma and impurity flows in the divertor region with spectroscopy in ASDEX-Upgrade [9] and DIII-D [10] or with probes as in Alcator C-Mod [11], TdeV [12], and ASDEX-Upgrade [13]. Yet results are still emerging within a growing body [14,15] of well documented divertor physics.

We present in this paper first results of parallel background plasma flow obtained with scanning Mach probes in the divertor region of DIII-D. The measurements are intrinsically local and obtained with high spatial resolution (2–3 mm). The geometry of the divertor (open) and the location of the probe at the divertor target plate allow access to divertor regions not previously studied in other devices.

## 2. Experimental set-up

The experiments have been performed on the DIII-D tokamak in discharges with plasma current  $I_p = 1.4$  MA, toroidal field  $B_t = 2$  T, flat-top duration of 5 s and chord-averaged density of  $0.5 - 1.0 \times 10^{20} \text{ m}^{-3}$ . The discharges are heated primarily by neutral beam injection at power levels of 4.5 MW. If a strong gas puff is introduced during the discharge, the divertor plasma temperature drops and the density increases as it detaches from the target plate.

A fast scanning probe array [16] is introduced vertically into the divertor plasma as shown in Fig. 1, with two of the tips configured as a Mach probe and two as a double probe. The magnetic configuration is the product of magnetic reconstruction performed by the code EFIT [17]. The Mach probe consists of two tips, aligned with the magnetic field, collecting saturation current. We utilize well-known models by Chung and Hutchinson [18,19] to interpret the measured Mach probe currents as plasma Mach number. The model includes viscosity and a self-consistent diffusive particle source. The plasma flow velocity is obtained by multiplying the local Mach number by the local sound speed  $c_s = (\gamma ZkT_e/m_i)^{1/2}$  where  $k$  is the Boltzmann constant,

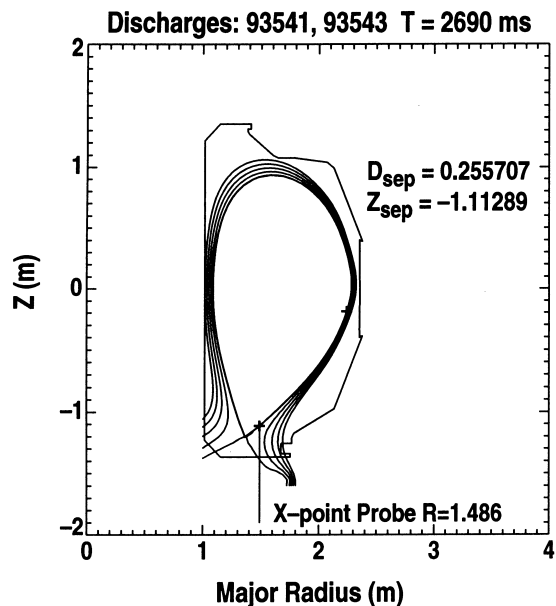


Fig. 1. The position of the scanning probe is superimposed on the reconstructed magnetic geometry for H-mode discharges. The probe moves along the outer SOL. The divertor Thomson scattering is in the same radial position as the probe at the Z-coordinates indicated by the points in Fig. 2.

$T_e$  and  $T_i$  are the electron and ion temperature,  $\gamma$  is the adiabatic constant and  $m_i$  is the ion mass. The voltage applied to the Mach tips is swept at 1 kHz to prevent sustained arcing, thus damage, to the tips when overheating occurs.

There are two sources of concern regarding the quality of the Mach measurement, the flow velocity to be derived from it and the probe data in general, namely: (1) the proximity of the probe to the divertor floor and (2) observed discrepancies between probe and Thomson scattering data during highly radiative discharges. We discuss the first concern here and the second in the “Results” section.

In a first approximation, the probe measurements can be disturbed if the connection length between the measuring tip and the divertor target plate is of the order of the probe collection length  $L_p$  or smaller. The plasma contained in the collection tube of the tip, filled by diffusion from surrounding plasma, is depleted by plasma flowing towards the divertor plate at a higher rate than it can be filled to reflect the properties of the main, unperturbed plasma. We estimate this critical distance [20],  $L_p$ , in terms of the probe area  $d^2$ , the local sound speed  $c_s$ , and diffusion coefficient  $D_\perp$ , to be  $L_p = d^2 c_s / 4D_\perp$  or 10–15 cm for DIII-D parameters ( $d^2 \sim 1 \text{ mm}^2$ ,  $D_\perp \sim 0.3 \text{ m}^2/\text{s}$ ,  $c_s \sim 7 \times 10^6 \text{ cm/s}$ ), which corresponds to a height of the probe from the floor of <1 cm. We observe ex-

perimentally that the measurements are perturbed for an elevation of <2 cm, which suggests that the diffusion coefficient used for the above estimate is too large or, equivalently, that the probe body plays a bigger role than expected and prevents the collection tube from filling up faster.

### 3. Results and discussion

We present in this paper results that address two issues: (1) the validity of the Mach measurement for a variety of conditions by comparing probe data and Thomson scattering data and (2) initial measurements of Mach number, flow velocity, saturation current and plasma potential in the divertor region, results pre-

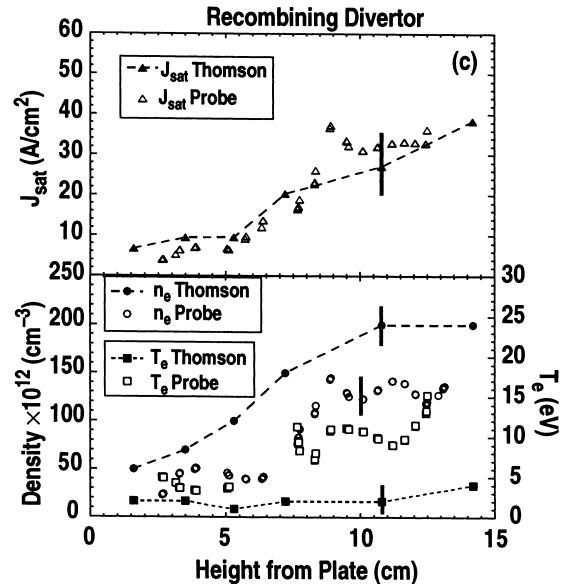
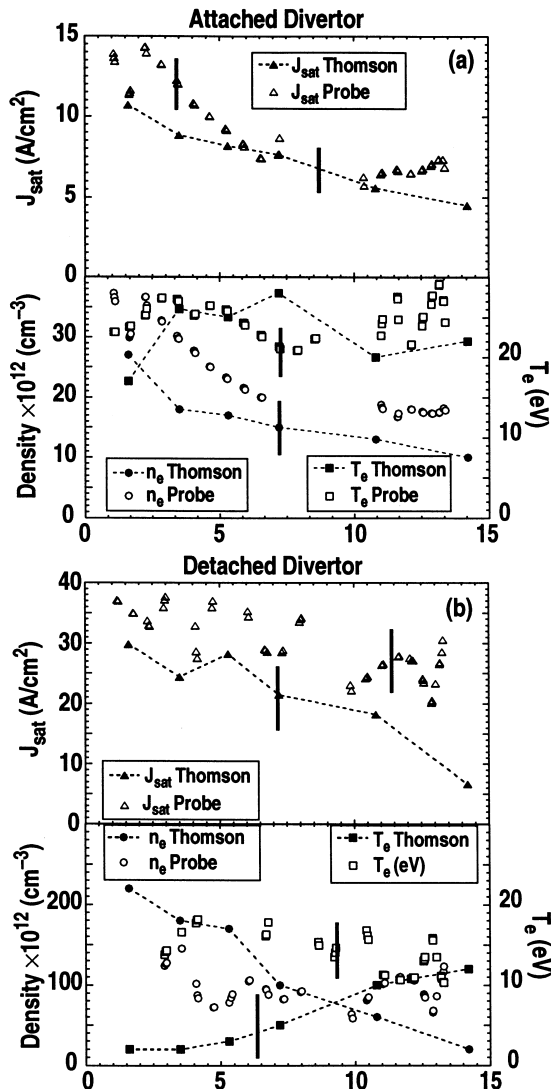


Fig. 2. Comparison of  $J_{sat}$  (upper panels),  $T_e$  and  $n_e$  (lower panels) measured by the probe (open symbols) and measured by Thomson scattering (filled symbols, dashed line) for (a) attached divertor plasma, (b) detached divertor plasma and (c) recombining divertor plasma.

sented in a coarse 2-D map from a multi-discharge divertor sweep. All experiments were performed in discharges such as those described in Section 2.

To validate the probe data, we obtained probe measurements for attached, recombining and detached divertor plasmas and compared them to Thomson scattering measurements taken at the same time. The geometry of the experiment is shown in Fig. 1.

The  $T_e$  and  $n_e$  measurements from the probe compare to Thomson measurements within 20% for attached plasmas as shown in Fig. 2(a) but differ for detached (Fig. 2(b)) or recombining (Fig. 2(c)) plasmas, where the probe measurements of  $T_e$  feature a variable degree of agreement with Thomson  $T_e$  and can be higher by factors of up to 2–3 [21], whereas the probe measurements of  $n_e$  are lower by 30%. A variety of experiments have seen this discrepancy and analyzed its origin [22,23]. A recent study has evaluated the existence of a high energy component in the DIII-D divertor [24] and its influence on the probe data, concluding that it is not an issue. This conclusion has been reached for floor probe data under similar DIII-D conditions as those shown in this paper. In this work, the discrepancy on the  $T_e$  measurements can be traced to high levels of fluctuations present in highly radiating divertors, which distort the measured  $I-V$  characteristic and tend to flatten the fit, therefore increasing the apparent temperature. An important fact is that the probe measurement of  $J_{sat}$  agrees with that inferred from Thomson data as seen in Fig. 2(a)–(c),

within 20% in all cases. The comparison of measurements suggests that the calculation of the sound speed in recombining or detached discharges, if inferred probe data, can be overstated by  $\sqrt{T_e^{\text{probe}}/T_e^{\text{Thomson}}}$  can be as high as 1.4–1.7. The result that  $J_{\text{sat}}$  is properly measured at all times assures us that the Mach number, dependent on the ratio of saturation currents from two pins, is always correct.

We have obtained a coarse 2-D map of various divertor plasma parameters, including Mach number and flow velocity, during experiments where the divertor

X-point is swept from smaller to larger major radius, in a shot-to-shot basis. The X-point sweep enables the scanning probe to investigate various regions of the divertor. We show the results of such a survey in Fig. 3 for attached divertor plasmas in a slowly ELMing (25 Hz) H-mode discharge as described in Section 2. The Mach number (Fig. 3(b)) and flow velocity (Fig. 3(c)) plots show that the flow velocity increases towards the target plate everywhere in the lower divertor as expected from sheath acceleration considerations but that flow stagnation is already apparent above the X-point in the

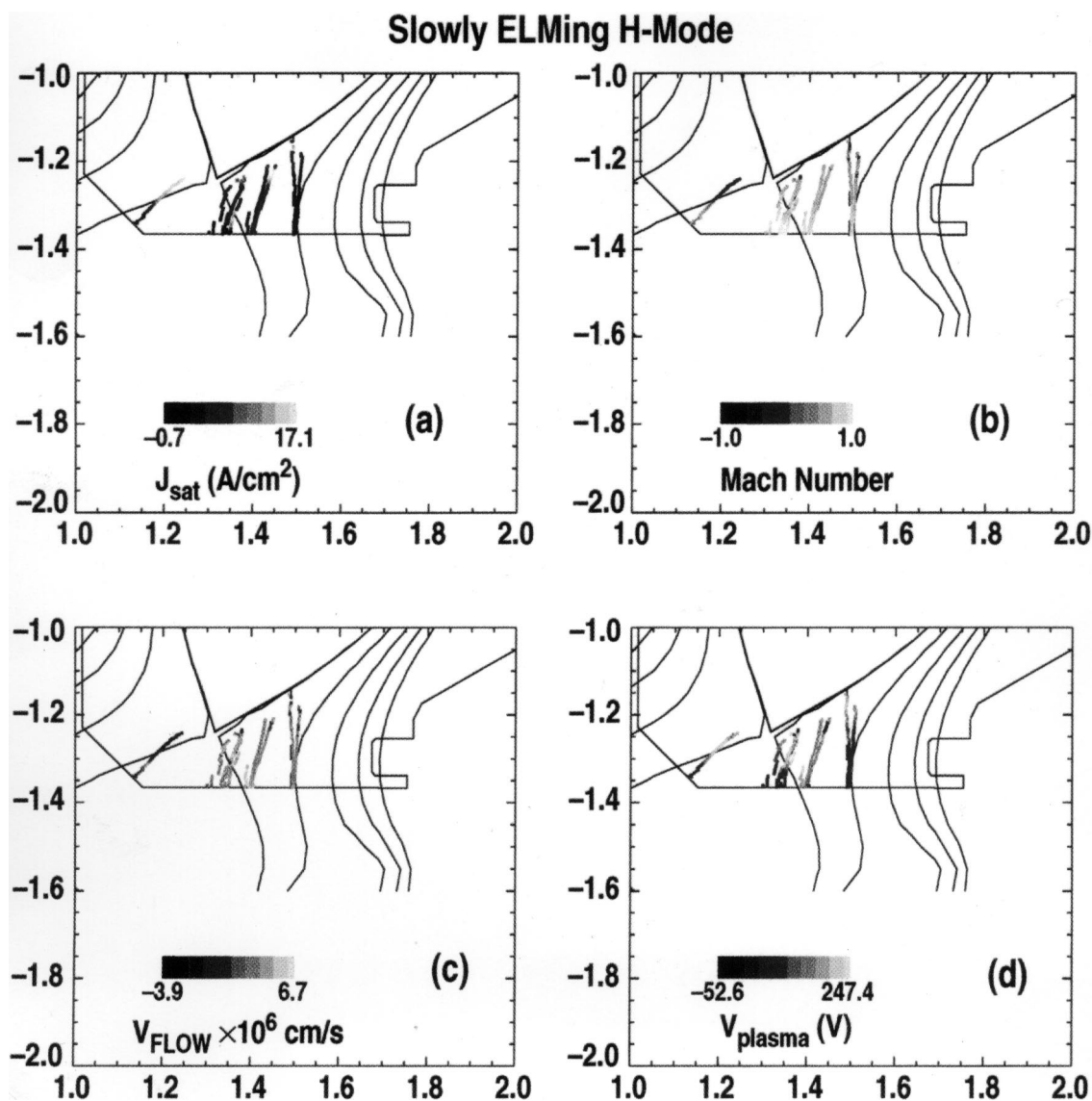


Fig. 3. 2-D plot built over the slowly ELMing phase of several discharges of (a) ion saturation current, (b) Mach number (positive means towards the divertor in the outer SOL) (c) flow velocity (positive means towards the divertor in the outer SOL) and (d) plasma potential, measured with respect to the vacuum vessel.

outer divertor leg. We also observe fine flow structures at the outer separatrix which correspond to flow reversal or slowdown. The slowdown of flow near the X-point and the outer separatrix should be related to pressure zones determined by ionization sources [7]. The ionization sources are due to neutral gas and carbon sources at the surfaces facing the plasma. The data shows that the plasma potential, measured with respect to the vacuum vessel, (Fig. 3(d)) features a large gradient when crossing the separatrix. These gradients (50–200 V/cm) will produce strong poloidal  $E \times B$  flows of the order of  $0.2 \times 10^6$ – $1 \times 10^6$  cm/s which are expected to affect the parallel flow patterns and produce considerable velocity shear that can stabilize turbulence in the divertor region. The plasma potential is calculated from the floating potential and the electron temperature measured by Thomson scattering in detached or recombining plasmas. The saturation current (Fig. 3(a)) in the divertor features sharp gradients at the inner and outer separatrix.

The fairly complex structure of plasma parameters in the divertor region has important implications for plasma and divertor performance. The flow of plasma determines particle and energy transport in the divertor by means of convection, thus affecting the divertor basic functions of particle and energy exhaust. The velocity of the background plasma is involved in the balance of forces acting on impurities, such as carbon, that contaminate the core plasma and reduce performance. Thus the impurity transport can be greatly determined by the background plasma convection as well.

#### 4. Conclusions

Double probe measurements of electron temperature and density in the divertor region agree well with Thomson scattering measurements for attached plasmas and tend to differ for detached and recombining plasmas, yet the particle flux agrees well within errors. A 2-D survey of the divertor, performed by a fast scanning probe array, determined that background plasma flows in the divertor region have a complex structure. The plasma flow velocity increases towards the divertor target plate as expected from free fall acceleration produced by the pre-sheath and it shows stagnation far away from the plate and the LCFS. The flow structure has important implications for particle and energy exhaust and thus will be the subject of more detailed studies in DIII-D.

#### Acknowledgements

Work supported by US Department of Energy under Grant No. DE-FG03-95ER54294, and Contracts DE-AC03-89ER51114, DE-AC04-94AL85000, and W-7405-ENG-48.

#### References

- [1] T.E. Evans, D.F. Finkenthal, Y. Loh et al., General Atomics Report GA-A22693, submitted to Plasma Phys. Control. Fusion.
- [2] M.J. Schaffer, D.G. Whyte, N. Brooks et al., Nucl. Fusion 35 (1995) 1000.
- [3] M.R. Wade, J.T. Hogan, J.T. Allen et al., Impurity enrichment studies with induced scrape-off-layer flow on DIII-D, submitted to Nucl. fusion.
- [4] T. Rognlien, J. Milosevitch, M. Rensink, G.D. Porter, J. Nucl. Mater. 196–198 (1992) 347.
- [5] G.D. Porter, DIII-D Team, Proceedings of 23rd European Conf. on Contr. Fusion and Plasma Physics, Kiev, Russia, vol. 20C, Part II, 1996, p. 699.
- [6] P.I.H. Cooke, A.K. Prinja, Nucl. Fusion 27 (1987) 1165.
- [7] M.A. Mahdavi, S.L. Allen, N.H. Brooks et al., Proceedings of 16th Int. Conf. on Fusion Energy, Montreal, IAEA-CN-64/A4-3, (1996), p. 397.
- [8] A.W. Leonard, M.A. Mahdavi, S.L. Allen et al., Phys. Rev. Lett. 78 (1997) 476.
- [9] J. Gafert et al., Plasma Phys. Control. Fusion 39 (1997) 1981.
- [10] R.C. Isler, N.H. Brooks et al., Normalized and reversed impurities flows in the DIII-D divertor, submitted to Phys. Plasmas.
- [11] B. LaBombard, J.A. Goetz, I. Hutchinson et al., J. Nucl. Mater. 241–243 (1997) 149.
- [12] B.L. Stansfield et al., J. Nucl. Mater. 220–222 (1995) 1121.
- [13] C.S. Pitcher, H.S. Bosch et al., Proc. 20th European Conf. on Control. Fusion and Plasma Physics I (1993) 1.
- [14] M.E. Fenstermacher, S.L. Allen, N.H. Brooks et al., Phys. Plasmas 4 (1997) 1761.
- [15] M.E. Fenstermacher, R.D. Wood, S.L. Allen et al., J. Nucl. Mater. 241–243 (1997) 666.
- [16] J.G. Watkins, J.G. Hunter et al., Rev. Sci. Instrum. 68 (1997) 373.
- [17] L.L. Lao, H. St. John et al., Nucl. Fusion 25 (1985) 1611.
- [18] K.S. Chung, I. Hutchinson, Phys. Rev. A 38 (1988) 4721.
- [19] K.S. Chung, I. Hutchinson, Phys. Fluids B 3 (1991) 3053.
- [20] P.C. Stangeby et al., Nucl. Fusion 30 (1990) 1225.
- [21] R.A. Moyer, J.W. Cuthbertson et al., J. Nucl. Mater. 241–243 (1997) 633.
- [22] R.D. Monk, J. Nucl. Mater. 241–243 (1997) 396.
- [23] N. Ezumi et al., Contrib. Plasma Phys. 38 (1998) S31.
- [24] J. Watkins et al., these Proceedings.